

Field and numerical investigation of filtered m-sequence pilots for Vibroseis acquisition

Joe Wong and David Langton

ABSTRACT

We conducted field tests using filtered m-sequences to control single land vibrators, and found that they potentially are just as effective as linear sweeps for use as Vibroseis pilots. We also evaluated the effectiveness of quasi-orthogonal filtered m-sequences driving land vibrators applied for simultaneous multi-sourcing. Results from the multi-sourcing survey indicated that time-domain filtered pilots produced deblended seismograms somewhat degraded by crosstalk interference originating from large-amplitude arrivals produced by adjacent and nearby vibrators. We conducted numerical simulations to show that, by filtering pure m-sequences in frequency domain instead of in time domain, we can obtain an improved set of quasi-orthogonal pilots for which crosstalk interference is much reduced. The improvement comes from retaining as much as possible the spectral energy that exists in pure m-sequences at frequencies between 4 and 100 Hz.

INTRODUCTION

High-resolution 3D seismic imaging often requires datasets with hundreds of millions or even billions of seismic traces. Acquiring such large datasets efficiently involves deploying as many geophones as possible. Acquisition productivity can be further enhanced by using multiple simultaneous sources. In both marine and land seismic surveys, this can be done with distance-separated seismic sourcing (DSSS). In this technique, several sources located at widely-spaced positions are activated synchronously or semi-randomly in time. Recorded seismic traces are the sum of the signals from all the sources, and before standard processing and imaging techniques can be applied, the summed data must be separated or deblended to yield ordinary common source gathers. The different time moveouts of events on the gathers of blended seismograms from the widely-spaced sources are exploited to separate the blended field data into unique common-source gathers associated with the individual sources (Beasley, 2008; Bouska, 2010; Bagaini and Yi, 2010).

In Vibroseis-based land surveys, deblending of data acquired with multiple simultaneous vibrators can be done successfully at the crosscorrelation step if the vibrators are driven by a set of quasi-orthogonal pilot signals. In the context of Vibroseis acquisition, a quasi-orthogonal set has the following properties:

- (1) Within a restricted window of time lags, the autocorrelation of any member in the set closely approximates the delta function.
- (2) Within the same time window, the crosscorrelation between any two different members in the set is very nearly zero.

Deblending of summed multi-source data using quasi-orthogonal pilots is effected at the crosscorrelation stage, and does not depend on differential time moveouts. Pilot signals that have been used in this way are variphase sweeps (Krohn et al., 2010), modified Gold codes (Sallas et al., 2011), and Galois codes (Thomas et al., 2010; 2012). Pecholcs et al. (2010) described a test 3D survey using 24 simultaneous vibrators controlled by variphase sweeps and modified Gold codes. Dean (2014) reviewed a variety of pseudorandom signals and their suitability as pilots for simultaneous multi-sourcing.

MAXIMAL LENGTH SEQUENCES

Maximal-length sequences, or m-sequences, are special mathematical signals that have step-function-like transitions between two values, -1 and 1. An m-sequence is characterized by its degree m , its fundamental length $L=2^m-1$, and its base period t_B . The sequence is periodic, repeating itself after a time equal to $L \cdot t_B$. Because the transition times are pseudorandom within each period, the autocorrelations of m-sequences are streams of triangular spikes that approximate delta functions; m-sequences are a type of pseudorandom binary signals, or PRBS. They are pseudorandom, because a truly random signal is infinitely long and aperiodic, and has an autocorrelation that displays a single large spike at zero lag).

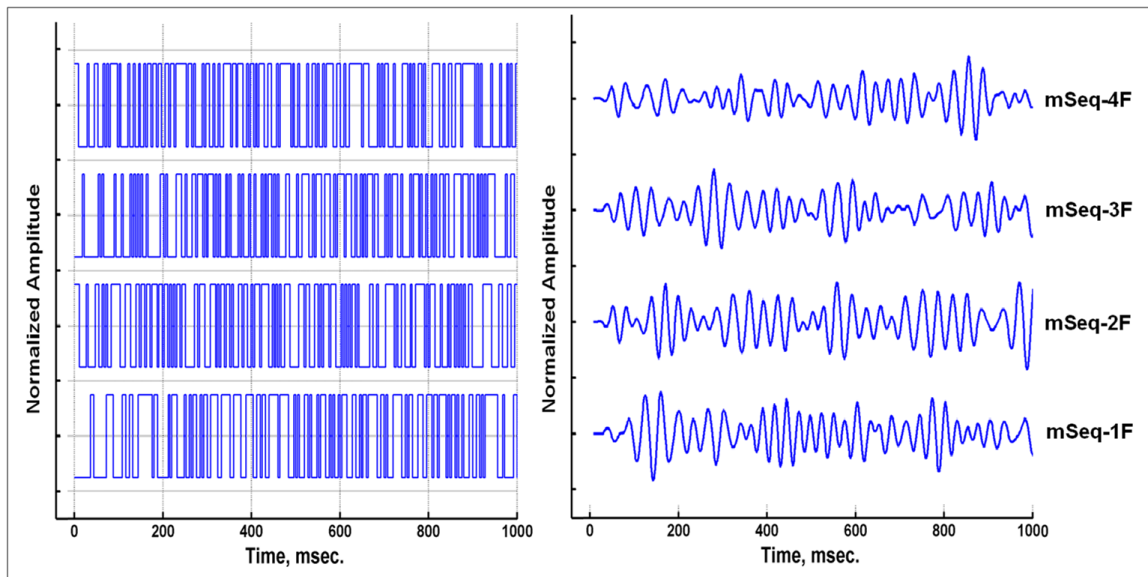


Figure 1: Left: shifted pure m-sequences mSeq-1 to mSeq-4. Right: time-domain filtered m-sequences mSeq-1F to mSeq-4F. Only the first 1000ms of the sequences have been plotted; the full periods of the sequences are 8188ms.

FILTERED M-SEQUENCES

Wong (2012a; 2012b) demonstrated theoretically how sets of shifted pure m-sequences are quasi-orthogonal, and therefore may be suitable for practical simultaneous multi-sourcing. However, initial attempts in field tests to drive land vibrators with the pure m-sequences shown on Figure 1 were unsuccessful. The square-wave-like transitions in the pure m-sequences are not compatible with the mechanical

characteristics of the hydraulic valves and positioning controls in land vibrators, and they cause rough and erratic operation of the vibrators.

Therefore, we modified the pure m-sequences to change the square-wave-like transitions to more moderate ramps. This was done by convolving the pure m-sequences with a realizable time-domain filter designed to reduce energy at frequencies below 20 Hz and above 100 Hz. The filtered shifted m-sequences are shown on the right side of Figure 1, and they are quasi-orthogonal for lag times in the range 0ms to 2040ms.

Single vibrator field results

Figure 2 shows in part the acquisition geometry used in our first field test. Four parallel receiver lines, approximately 5800m long and separated by 200m, were laid out with geophones placed at 50m intervals along each line. A single vibrator V1 was placed about 5m from receiver line Rx-2. We then recorded data for all four receiver lines with V1 driven first by a conventional linear sweep pilot, and then by a filtered m-sequence pilot (mSeq-1F from figure 1).

The linear sweep pilot covered 4Hz to 140Hz with a sweep time of 16 seconds and end tapers of 300ms. For the filtered m-sequence pilot, we swept with two full cycles for a duration of 16.376 seconds. We listened and recorded for 22 seconds for both types of pilots, digitizing receiver signals with a 2ms sampling interval. Seismograms were extracted from the raw field data post-survey by crosscorrelating them with the pure m-sequences or with the linear sweep pilot.

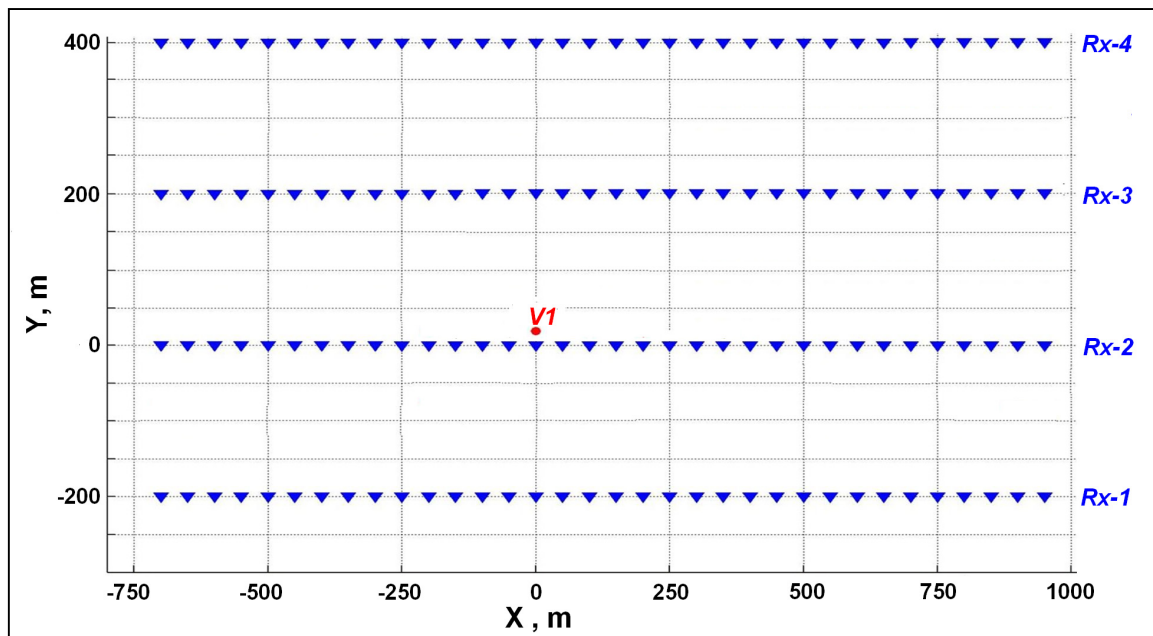


Figure 2: Field configuration for testing a single vibrator V1 driven by a standard linear sweep, and then by an m-sequence pilot (2 cycles of 8.188 seconds each). Listen time in both cases is 22 seconds. The four receiver lines Rx-1 to Rx-4 are about 5800m long. Receivers (represented by blue triangles) are located at 50m intervals.

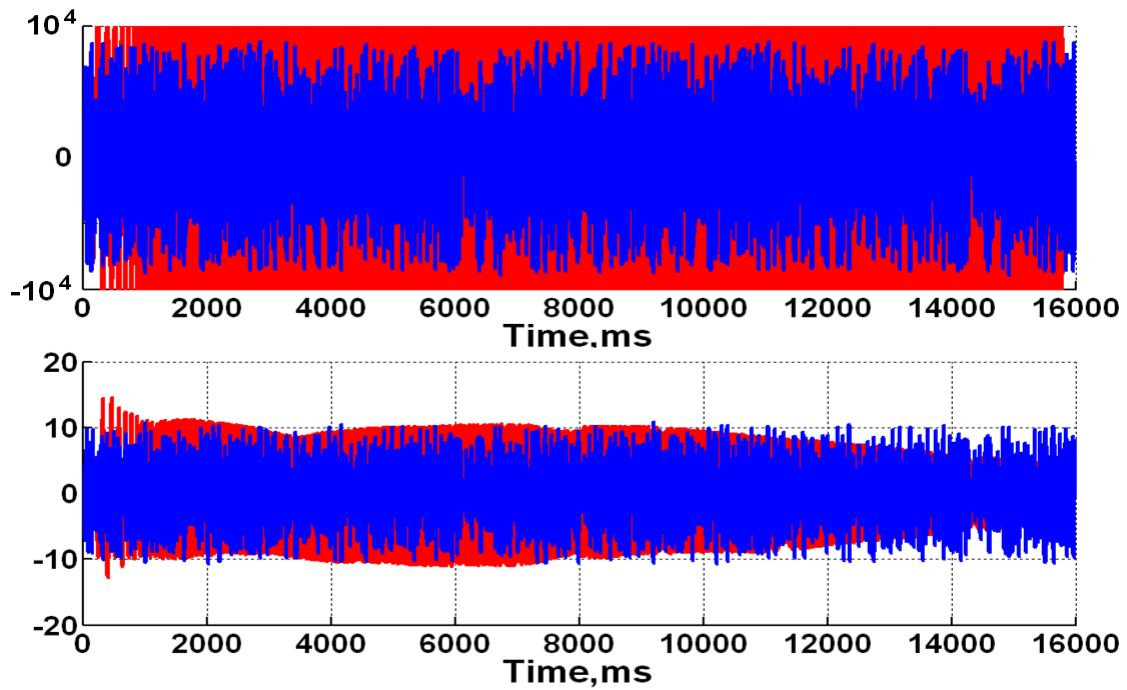


Figure 3: Pilots (TREF- top) and ground force (GF- bottom) signals for single vibrator test. Red is the linear sweep; blue is the filtered m-sequence pilot.

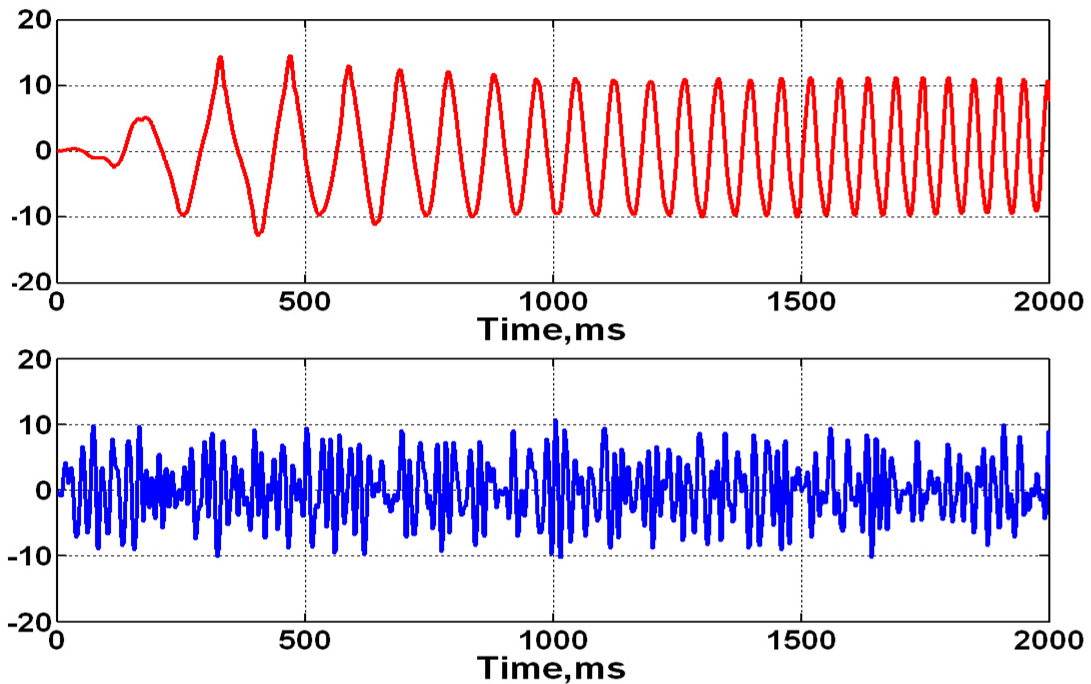


Figure 4: Expanded view of GF (ground force) signals for the single vibrator test. Red is the linear sweep GF; blue is the filtered m-sequence GF. Note the distortion on the linear sweep GF.

The linear sweep and filtered m-sequence signals are shown on Figure 3 in red and blue respectively. The linear sweep TREF had been set to 100% of the maximum allowed by the vibrator controller, while the m-sequence TREF had been set to 70%. However, as a precaution to minimize possible damage to the vibrator, the controller output settings were adjusted so that the both GF outputs were approximately equal at 70% of the rated maximum.

Figure 4 plots the first 2000ms of the recorded ground force signals generated by the linear sweep and the m-sequence pilot. The vibrator controller settings were adjusted so that both GF outputs (estimated by the weighted sum of the measured accelerations on the base plate and reaction mass of the vibrator) are nearly equal. The amplitude spectra of the ground force signals for both types of pilots are plotted on figure 5.

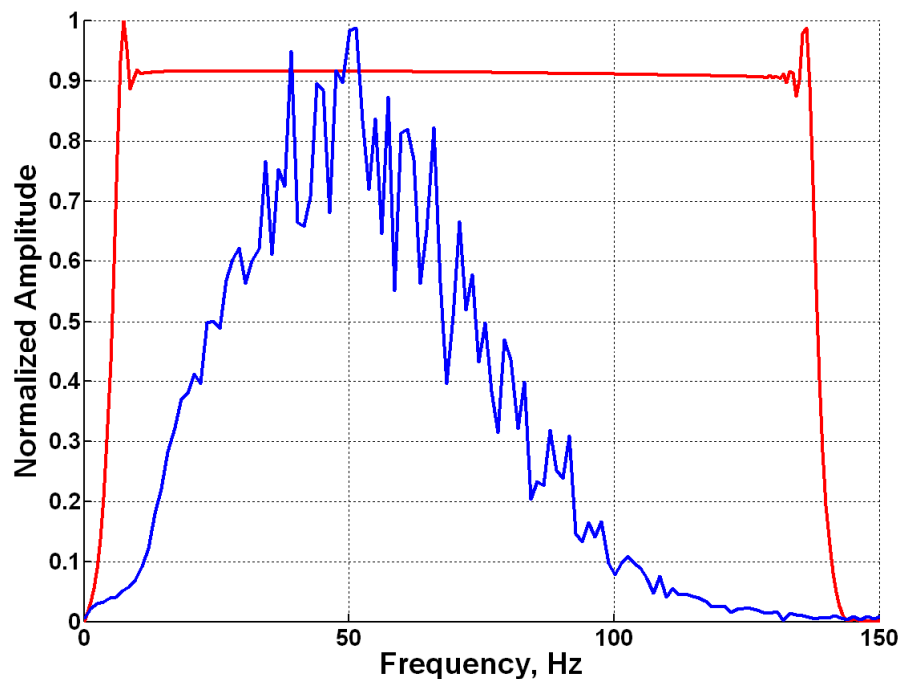


Figure 5: Amplitude spectra of ground force signals for single vibrator test. Red is the linear sweep GF; blue is the filtered m-sequence GF.

Figure 6 plots the autocorrelations of the linear sweep ground force and the filtered m-sequence ground force using linear scales, while Figure 7 plots them using a decibel scale. The maximum amplitude of the linear sweep autocorrelation is about twice that of the filtered m-sequence autocorrelation, and the negative side lobes are smaller relative to the correlation peak. These differences reflect the difference in the amplitude spectra as shown on figure 5. However, by adjusting the filtering of the pure m-sequence, we can mitigate these differences if we so desire (see below, Numerical Simulations). Relative values of the filtered m-sequence autocorrelation at non-zero lag times are important, because they affect details appearing in the seismograms extracted from raw uncorrelated field data by crosscorrelation with the TREF or GF forces.

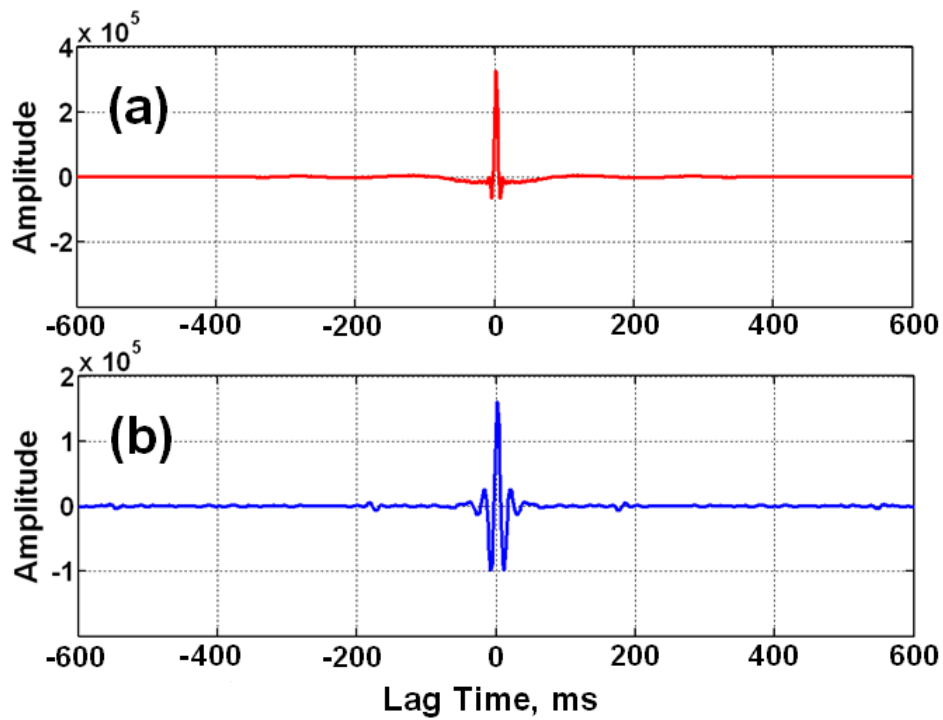


Figure 6: Amplitudes of autocorrelations for: (a) linear sweep ground force; (b) filtered m-sequence ground force.

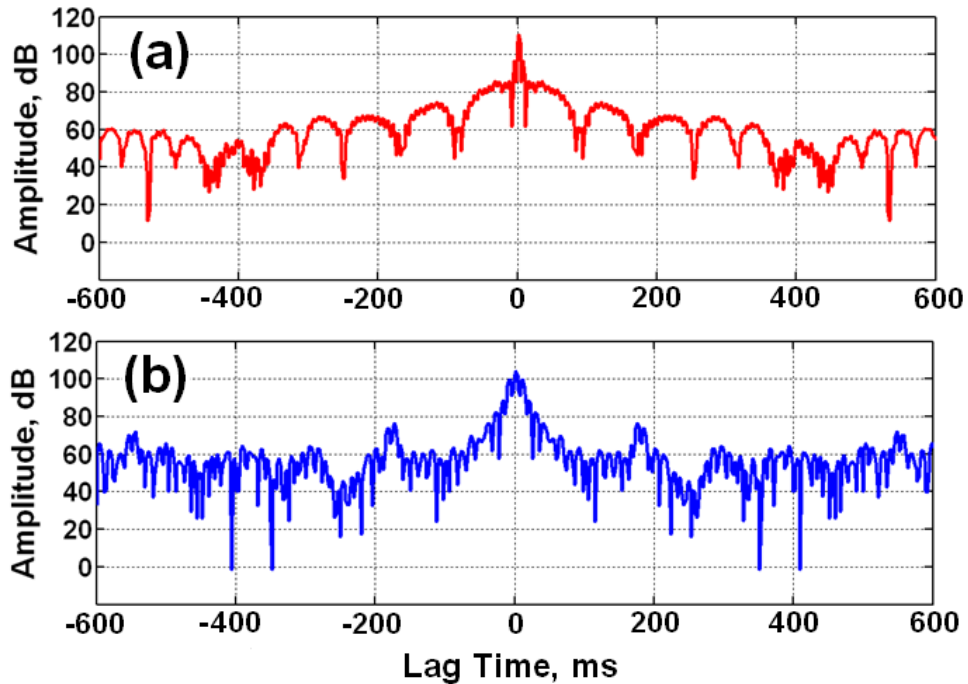


Figure 7: Autocorrelation amplitudes in decibels for (a) linear sweep ground force; (b) filtered m-sequence ground force. Note the local peaks or side lobes on the m-sequence autocorrelation near (+/-) 280ms and (+/-) 560ms.

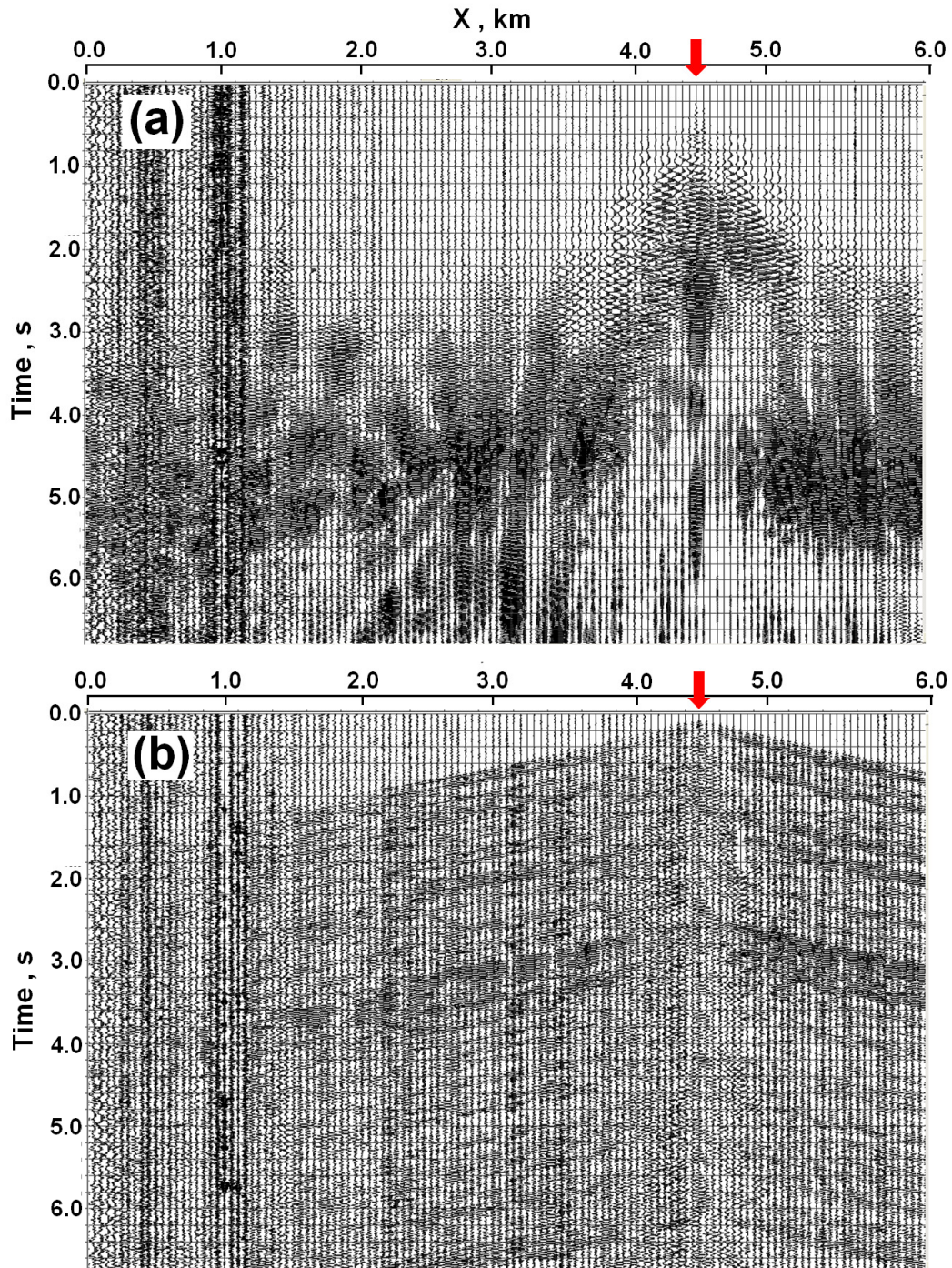


Figure 8: (a) Trace-normalized CSGs for receiver line Rx-2, recorded using a single vibrator (a) driven by the linear sweep pilot, and (b) driven by the filtered m-sequence pilot.

Figure 8 displays raw uncorrelated data recorded for the receiver line offset 5m from vibrator V1. The durations of the recorded raw data traces are equal to the listen time of 22 seconds, but the figure displays only the first 6.8 seconds. We can see the appearances of the uncorrelated common sources gathers (CSGs) produced by the linear sweep and m-sequence pilots are dramatically different. The uncorrelated CSG produced by the

linear sweep pilot exhibit little spatial or temporal coherence, with frequencies and amplitudes changing without any apparent pattern. On the other hand, the uncorrelated CSG produced by the m-sequence pilot shows strong amplitudes for the full duration of the traces, with a distinct chevron pattern following the time moveout associated with the first arrivals.

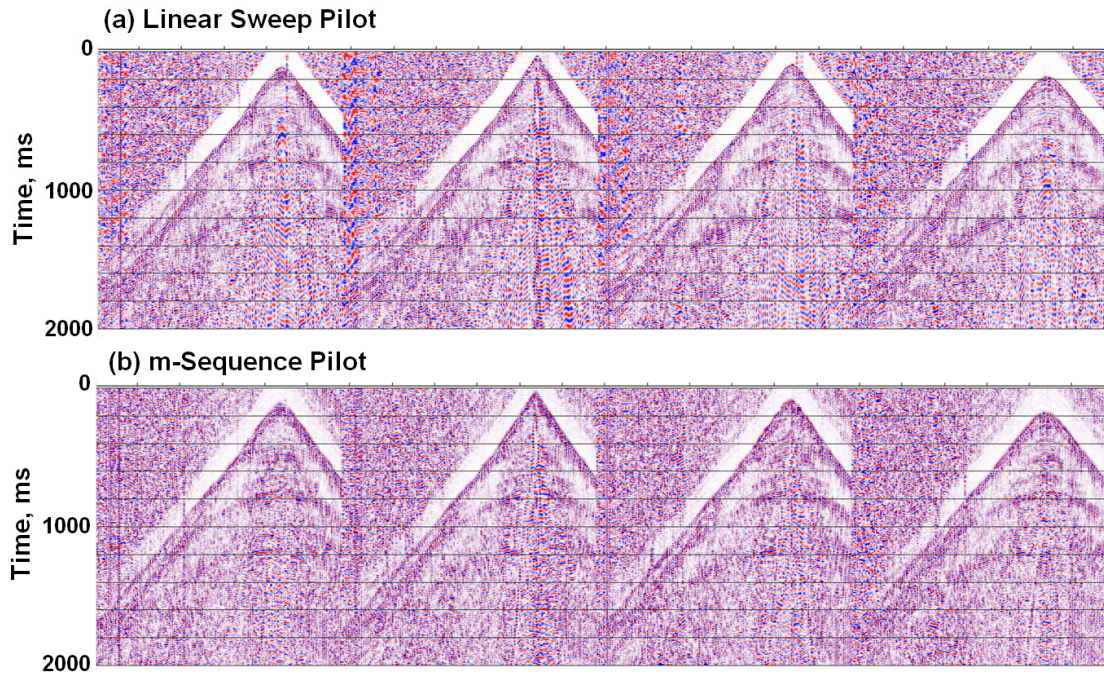


Figure 9: (a) Correlated CSGs for four receiver lines recorded using a single vibrator (a) driven by the linear sweep pilot, and (b) driven by the filtered m-sequence pilot. These unfiltered seismograms are plotted with a 200ms AGC window.

Crosscorrelation with the appropriate TREF signals produced the impulsive seismograms plotted on Figure 9. Note the good similarity between the linear sweep and the m-sequence CSGs for all four receiver lines. The CSGs on Figure 9(b) produced with m-sequence pilots show weak artifacts that partially interfere with the weaker reflections. These artifacts resemble multiples of the direct arrival, and are caused by weak late-time side lobes in the autocorrelation of the filtered m-sequence ground force (see Figure 7). They also may be related to small harmonic distortions and/or nonlinearities in the mechanical responses of the vibrators. The ground-roll noise associated with the m-sequence seismograms seems to have lower relative amplitudes than the ground-roll noise associated with the linear sweep seismograms.

On Figure 10(a), we compare the maximum amplitudes of the linear sweep seismograms to the maximum amplitudes of the m-sequence seismograms for all four receiver lines. With a vertical scale of 0 to 100 dB, we see little difference in the maximum amplitudes. On Figure 10(b), where the ratios of maximum amplitudes are

plotted, we see that the linear sweep seismograms have maximum amplitudes about 2 to 6 dB stronger than those of the m-sequence seismograms.

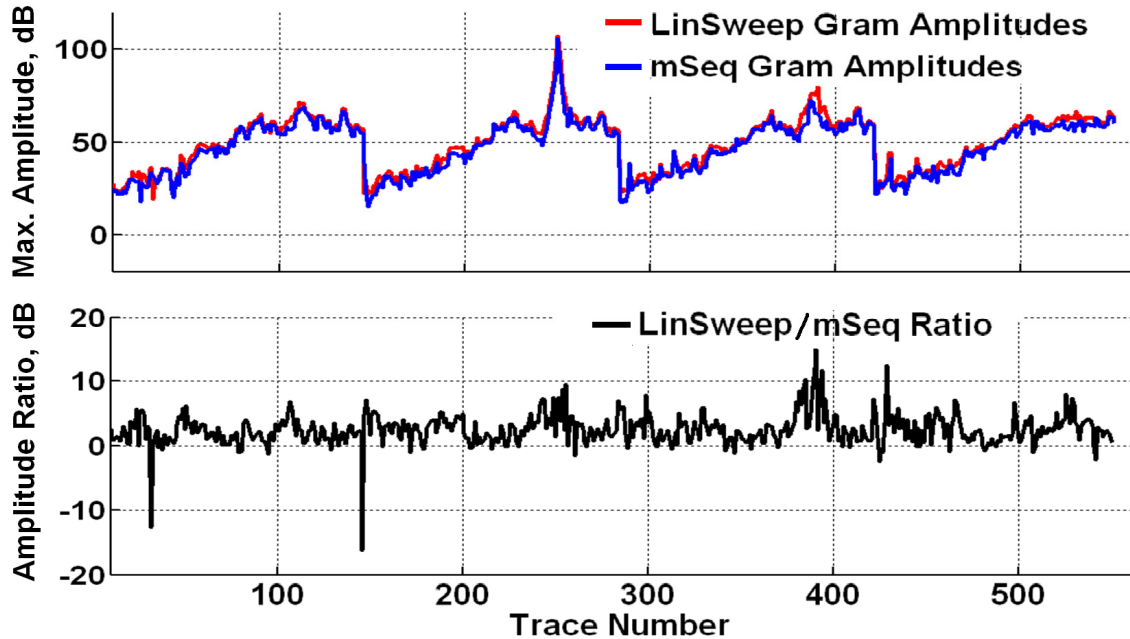


Figure 10: Top: comparison of maximum amplitudes of linear sweep seismograms and m-sequence seismograms. Bottom: ratio of linear sweep maximum amplitudes to m-sequence maximum amplitudes.

Concern has been expressed about the lower amplitudes produced with the filtered m-sequence pilot relative to those produced by the linear sweep pilot. While increased maximum amplitudes enhance the signal-to-noise ratios (SNRs) of seismograms if the noise is random, it has no effect on SNRs if the noise is source-related. Examples of source-related noise are ground roll and incoherent events caused by geological scattering. In any case, the maximum amplitudes of m-sequence seismograms can be increased by vertical stacking, which can be done inexpensively by exploiting the periodicity of m-sequences.

The single-vibrator experiment yielded common-source seismograms that are not significantly different regardless of whether they were generated by the linear sweep pilot or by the m-sequence pilot. This suggests that filtered m-sequences are potentially just as effective as linear sweeps for controlling land vibrators in single operation.

Two vibrators driven simultaneously by two m-sequence pilots

Figure 11 is a schematic representation of the test survey for acquiring data with two vibrators running simultaneously. We placed vibrators V1 and V2 200m apart and located them about 5m from receiver line Rx-2. Using mSeq-1F as the pilot for vibrator V1 and mSeq-2F as the pilot for vibrator V2, we recorded blended uncorrelated data. Figure 12 is a plot of the blended raw data for the near-offset receiver line Rx-2. Note the strong low-frequency ground roll noise at those receivers closest to the vibrators.

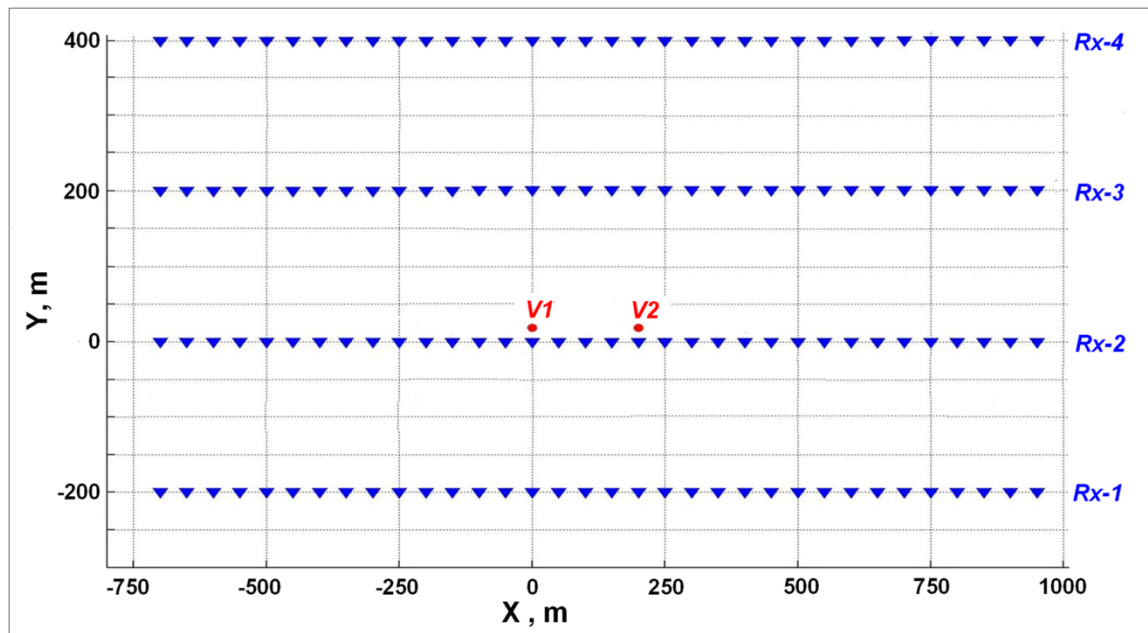


Figure 11: Field configuration for testing two vibrators V1 and V2 driven simultaneously by two quasi-orthogonal m-sequence pilots. The vibrators are separated by 200m. The four receiver lines Rx-1 to Rx-4 are about 5800m long.

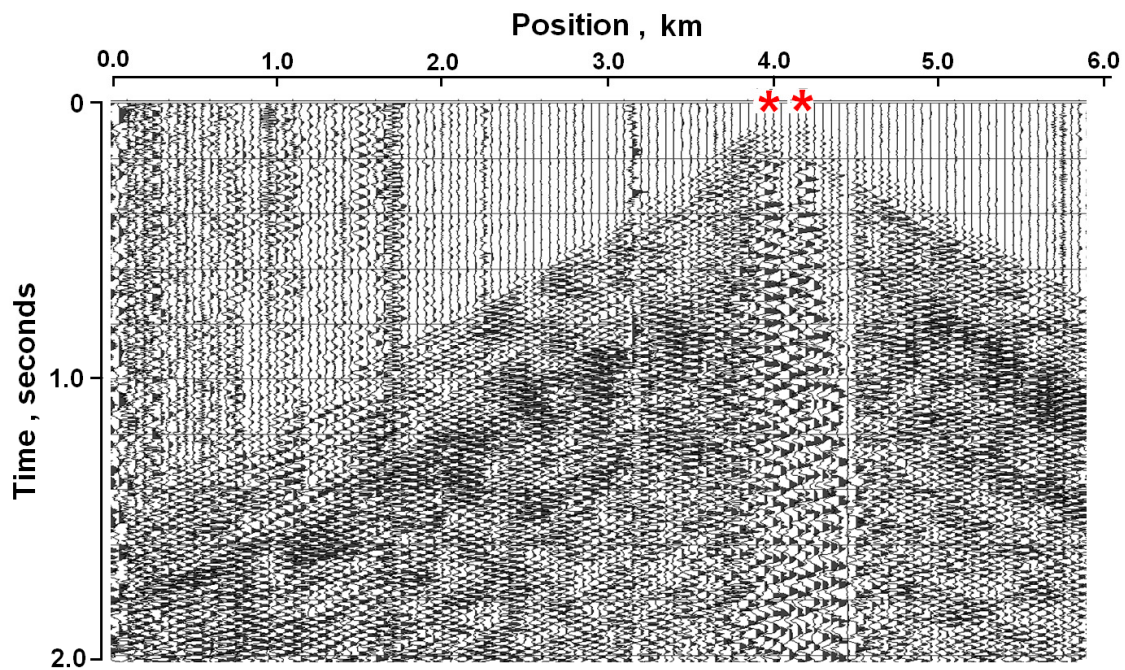


Figure 12: Trace-normalized plot of raw uncorrelated field data recorded with vibrators V1 and V2 controlled by m-sequence pilots by the filtered m-sequences mSeq-1F and mSeq-2F, respectively, and running simultaneously. The red stars denote the positions of the two vibrators.

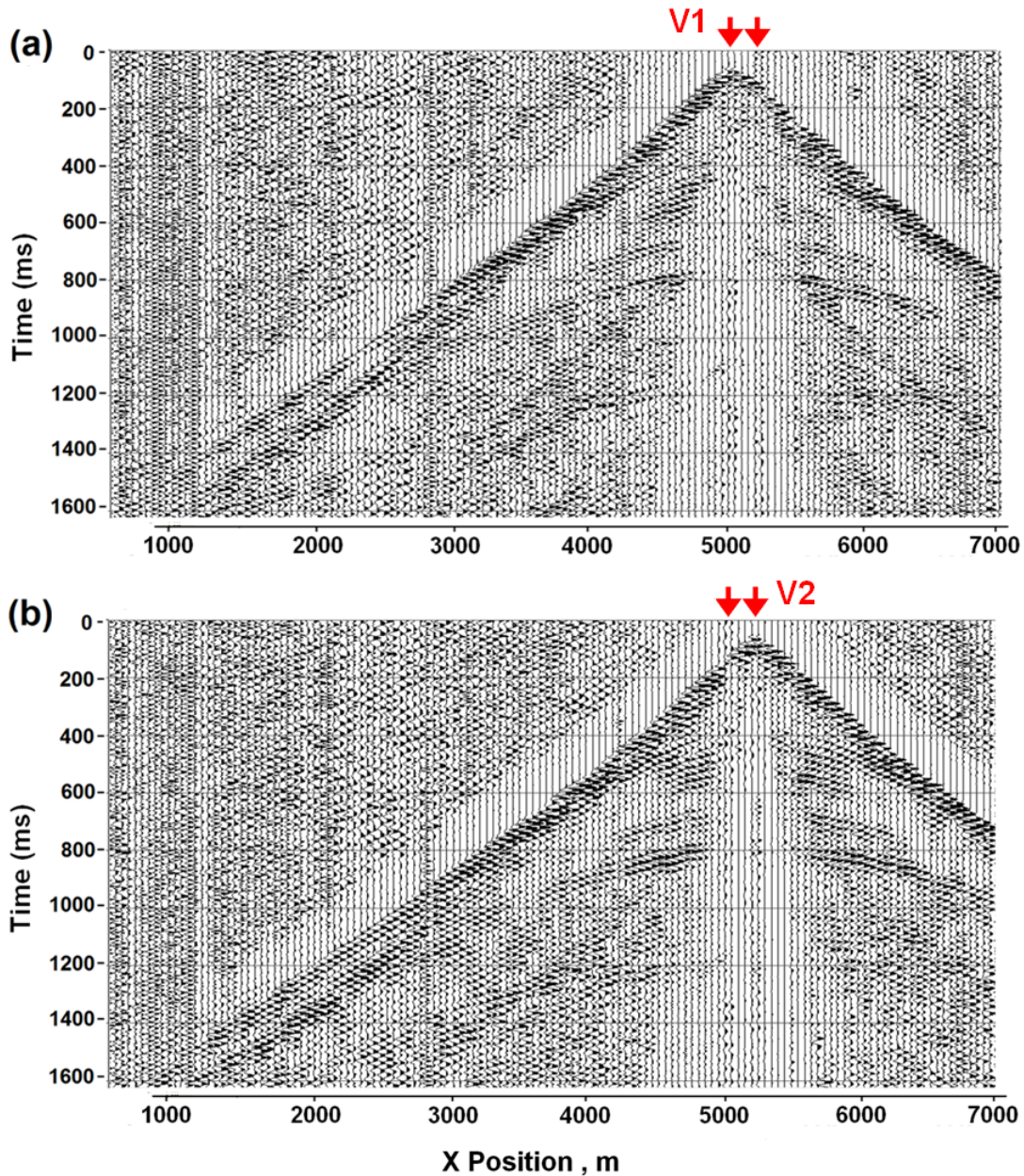


Figure 13: AGC plots of debledned seismograms: (a) for vibrator V1; (b) vibrator V2. Bandpass filtering has been applied to reduce ground roll noise.

We extracted debledned common-source gathers (CSGs) associated with vibrators V1 and V2 by crosscorrelating the raw data with the pure m-sequences mSeq-1 and mSeq-2. These are plotted with an AGC window of 200ms on Figures 13(a) and 13(b) after attenuating the low-frequency surface-wave arrivals with a bandpass filter (15Hz-30Hz-100Hz-200Hz) to emphasize the reflections from subsurface interfaces. All the reflections that appear on the CSG acquired with the linear sweep pilot (Figure 9) are present on the debledned CSGs acquired with the filtered m-sequence pilots. As on Figure 9, the reflections near 800ms and 1200ms on the debledned gathers are somewhat degraded by weak artifacts with time moveouts that run parallel to the first arrivals.

We reduced interference from the weak artifacts using processing steps that included NMO/DMO alignment, trim statics, signal enhancement, and trace interpolation. Figure 14 displays the processed results for the V1 and V2 gathers extracted from the blended data. A similarly processed CSG of data acquired using vibrator V2 controlled by the linear sweep pilot is plotted on the left side of Figure 15. After processing, reflections on data acquired simultaneously with the m-sequence pilots are visually very similar to reflections on data recorded with the linear sweep pilot.

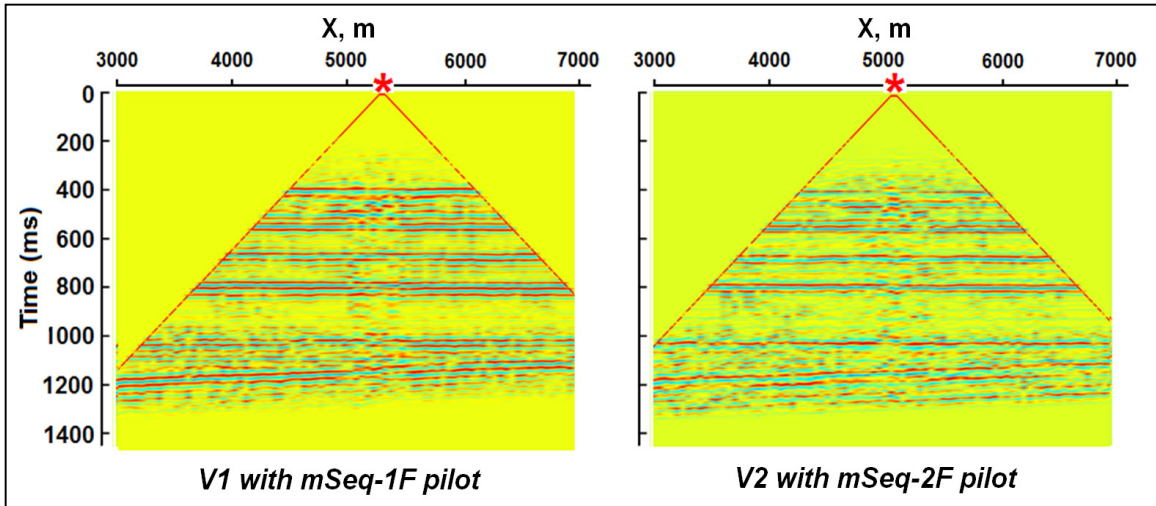


Figure 14: AGC plots of processed deblended CSG for vibrators V1 and V2. Right and left red stars indicate positions of the two vibrators V1 and V2.

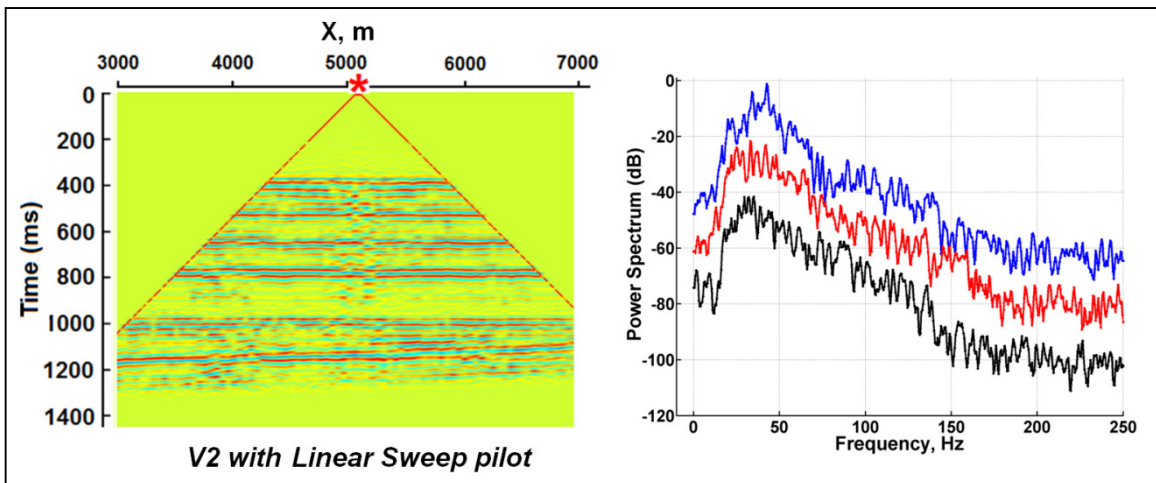


Figure 15: Left: Processed CSG acquired with single vibrator V2 driven by the linear sweep of Figures 3 and 4. Right: averaged power spectra of the processed gathers shown on Figure 14 and the processed linear sweep CSG. Blue = mSeq-1F data; red = mSeq-2F data, black = linear sweep data. The spectra have been displaced by 20dB for clarity of display.

The right side of Figure 15 compares the amplitude spectra (averaged over all traces) of the CSGs on Figure 14 and the processed linear sweep CSG plotted on the left side. We see that, while spectra of the GF signals of the linear sweep and the m-sequence pilots are very different (see Figure 5), the spectra for the processed field seismograms from the linear sweep pilot and from the m-sequence pilots are quite similar.

Four vibrators driven simultaneously by four m-sequence pilots

Figure 16 is a schematic representation of the acquisition geometry for field-testing four vibrators running simultaneously. The four vibrators, V1, V2, V3, and V4 were along a line about 5 meters away from receiver line Rx-2.

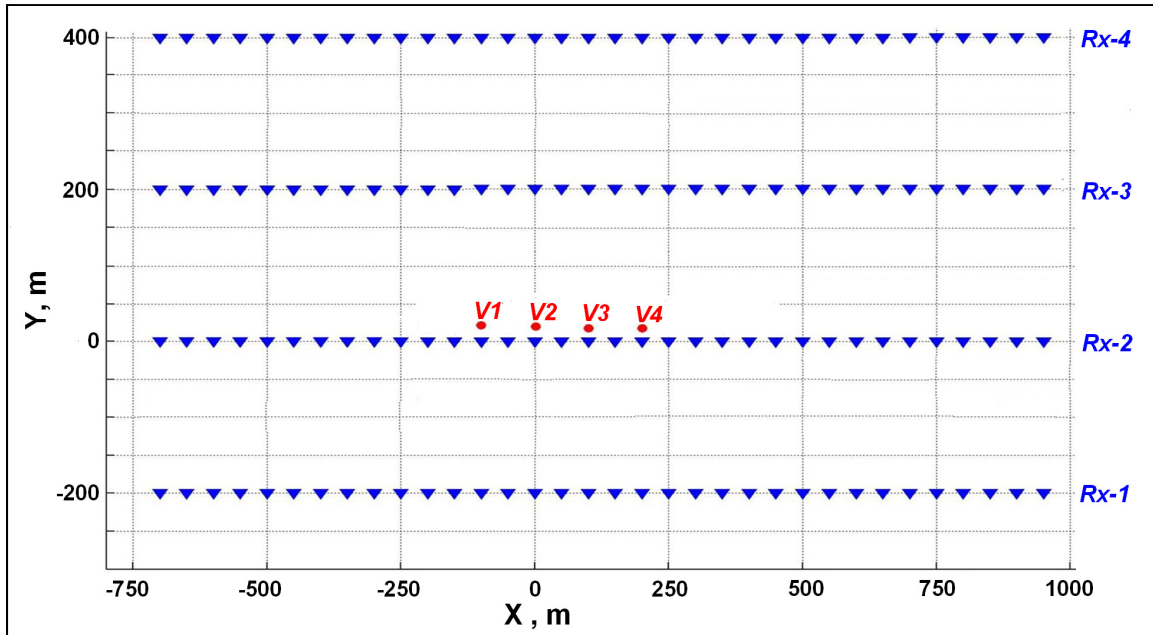


Figure 16: Field configuration for testing four vibrators driven simultaneously by four quasi-orthogonal m-sequence pilots. The spacing between adjacent vibrators is 100m. The four receiver lines Rx-1 to Rx-4 are about 5800m long.

Four filtered m-sequences (mSeq-1F, mSeq-2F, mSeq-3F, and mSeq-4F from Figure 1) were used as pilots for the four vibrators. Two full cycles of each pilot were used for a total sweep time of 16.376 seconds. The listen time was 22 seconds, sampling time was 2ms, and we recorded data for all four receiver lines. Here, we will show results only for receiver lines Rx-1 and Rx-2.

Figure 17 is a trace-normalized plot of blended uncorrelated data recorded for the 5m offset receiver line Rx-2. Note the strong low-frequency ground roll noise at receiver positions closest to the vibrators. We extracted deblended common-source gathers (CSGs) for each of the four vibrators by crosscorrelating the raw data with the appropriate m-sequence pilots. These are plotted with an AGC window of 200ms on

Figures 18 to 21 after attenuating the low-frequency surface-wave arrivals with a bandpass filter (15Hz-30Hz-100Hz-200Hz).

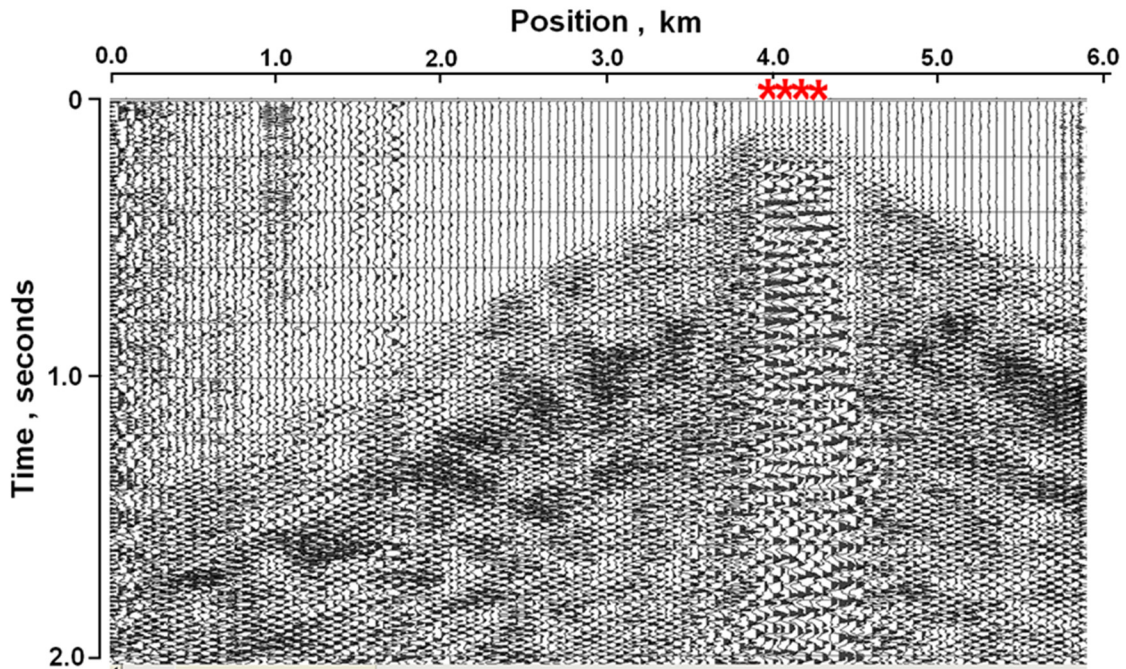


Figure 17: Trace-normalized plot of raw uncorrelated field data recorded for four simultaneous vibrators controlled by four quasi-orthogonal m-sequence pilots.

On Figures 18 to 21, we see clear first arrivals and hyperbolic reflections with apexes at about 800ms and above. Reflections with apexes near 1200ms are visible, but they are somewhat degraded by weak artifacts and by weak crosstalk interference, particularly for the near-offset line. Crosstalk originates from high-amplitude direct arrivals and strong surface waves coming from adjacent and nearby vibrators.

Effective deblending depends on the ability of the filtered m-sequences and their quasi-orthogonality property to separate weak body-wave signals from the very strong direct arrivals and surface-wave signals. The separation using crosscorrelation can be very good, but practically, it is never 100% effective. Some receivers on the 5m–offset line are extremely close to the vibrator sources. For these receivers, the ratios of strong direct-arrival and surface-wave amplitudes from adjacent and nearby sources to the weaker amplitudes from the source of interest are very large. The crosstalk after deblending remains visually discernible. The crosstalk is much reduced for the 200m–offset receiver line, because the ratios between amplitudes produced by all the sources are much closer to one for all receivers.

We can reduce the crosstalk between different vibrator sources simply by reducing the distances between the vibrators. For example, on Figure 16, if we reduce the source-to-source separation from 100m to 50m we decrease (for all receivers) the disparity in the distances to the nearest vibrator and farthest vibrators. This also reduces the disparity in

amplitudes arriving from the closest and farthest vibrators. The reduced amplitude disparity means less crosstalk after deblending.

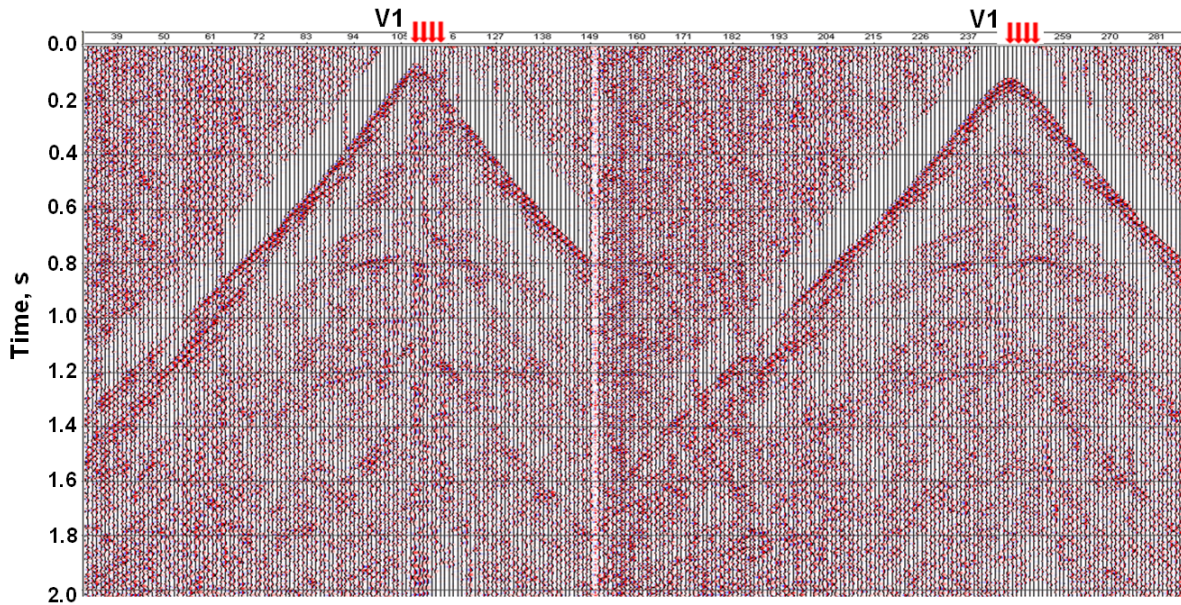


Figure 18: AGC plot of bandpass-filtered seismograms for vibrator V1 extracted from the blended raw field data. Left: for receiver line offset ~5m from source. Right: for receiver line offset 200m from source.

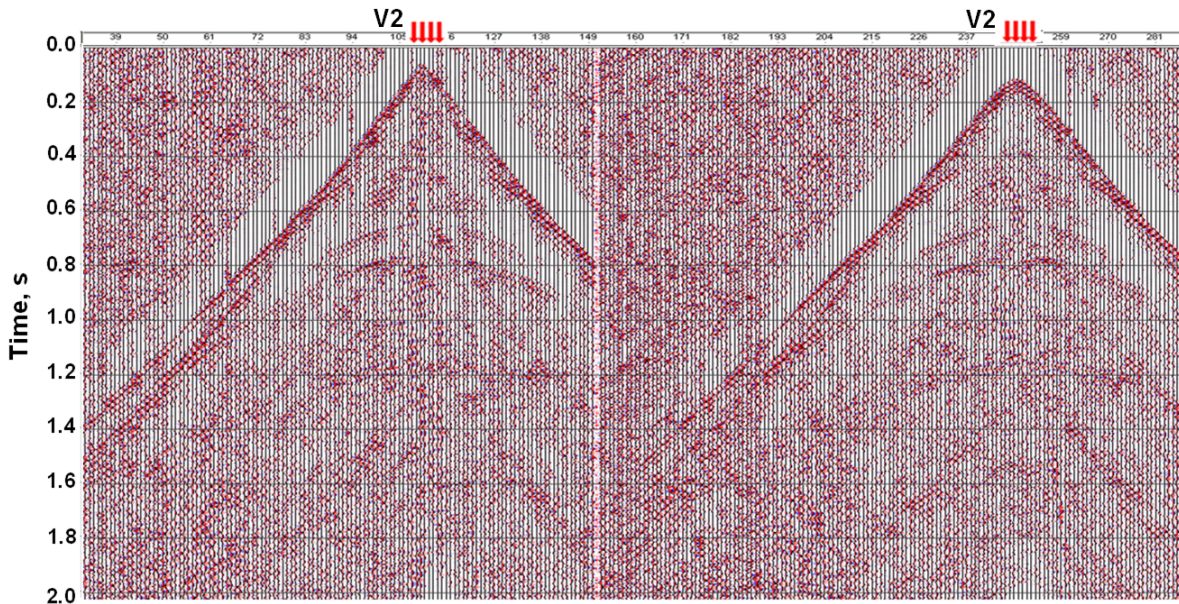


Figure 19: AGC plot of bandpass-filtered seismograms for vibrator V2 extracted from the blended raw field data. Left: for receiver line offset ~5m from source. Right: for receiver line offset 200m from source.

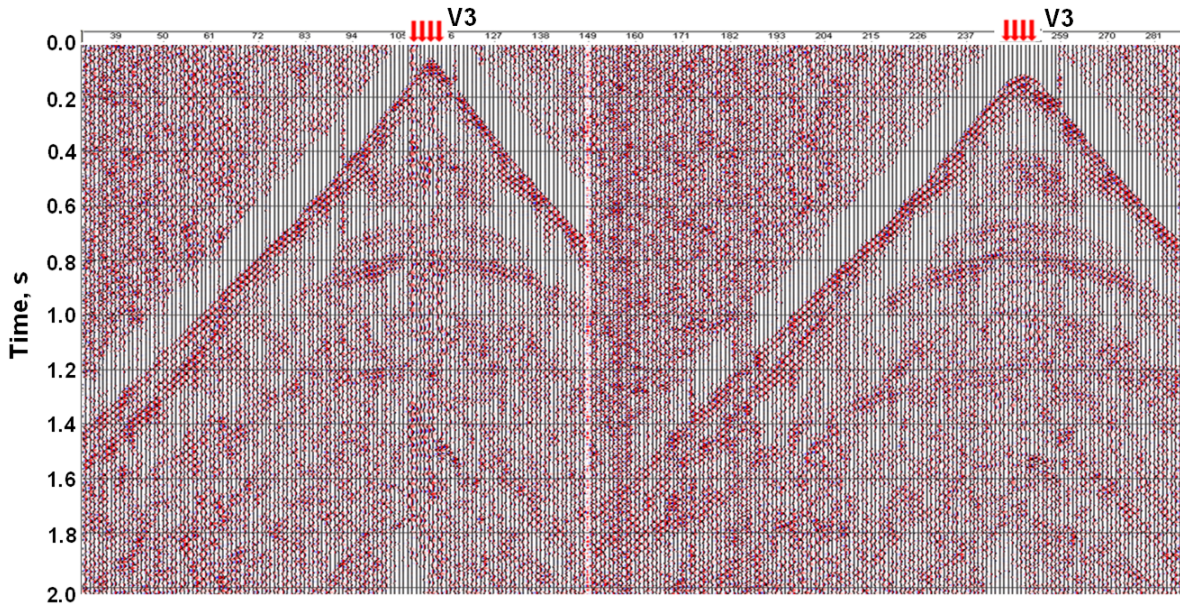


Figure 20: AGC plot of bandpass-filtered seismograms for vibrator V3 extracted from the blended raw field data. Left: for receiver line offset ~5m from source. Right: for receiver line offset 200m from source

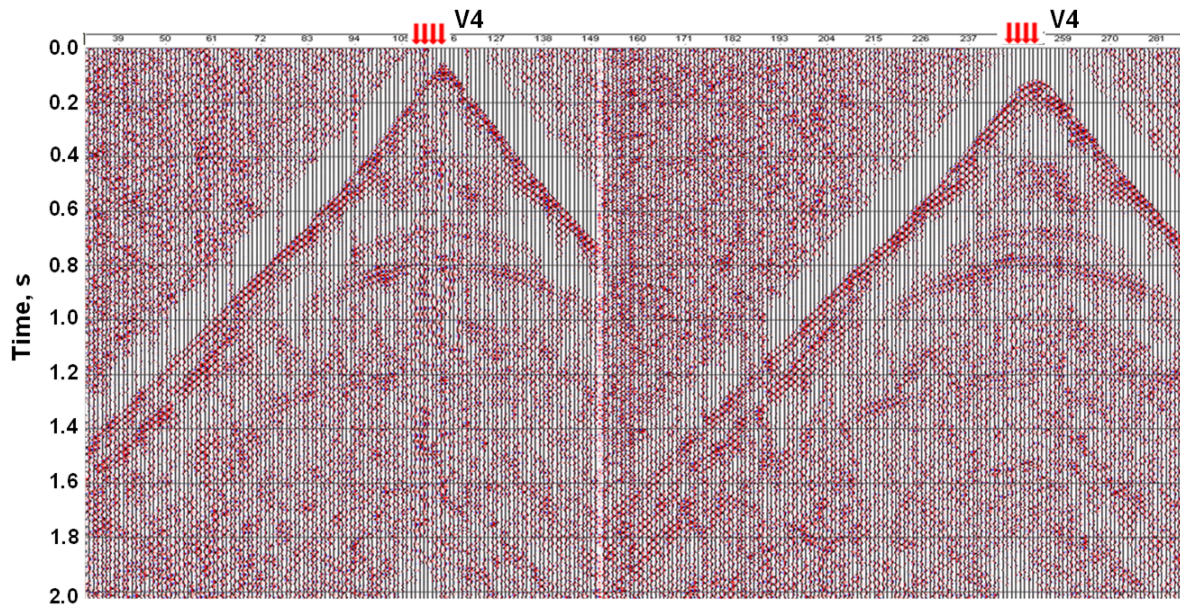


Figure 21: AGC plot of bandpass-filtered seismograms for vibrator V4 extracted from the blended raw field data. Left: for receiver line offset ~5m from source. Right: for receiver line offset 200m from source.

NUMERICAL SIMULATIONS

The deblended CSGs on Figures 18 to 21 indicate that the particular set of time-domain filtered m-sequences performed reasonably well when applied for simultaneous multi-sourcing. However, we would like further decrease the still visible crosstalk, weak though it may be. In this section, we use numerical simulations to explore how we can change the filtered m-sequences to achieve a further improvement in their deblending capability.

The spectrum of the time-domain filtered m-sequences used in the field tests is shown on Figure 22(a) in red. The blue line is the spectrum of the pure, unfiltered m-sequences. For seismic exploration, the important frequency range is about 4 to 100Hz, and in this range the time-domain filter has eliminated much of the spectral energy that exists in the original pure m-sequences. Figure 22(b) plots the auto- and crosscorrelations of the time-domain filtered m-sequences. Note that crosscorrelation values are relatively large at about -36 to -40 dB for all lag times.

Instead of using a time-domain filter to moderate the square-wave transitions on pure m-sequences, we can use a bandpass filter in frequency domain to do the same thing. Frequency-domain filtering enables us to have more control on the final spectral content of the filtered m-sequences. The plots on Figure 23(a) indicate that in the frequency range 5 to 250 Hz we have retained almost all of the spectral energy of the pure m-sequences after the application of a [5-10-160-250] Hz Ormsby filter in frequency domain. Figure 23(b) displays the auto- and crosscorrelations of the frequency-domain filtered m-sequences.

Comparing Figures 22(b) and 23(b), we see that the off-peak autocorrelation values of the frequency-domain filtered m-sequences are lower by about 45dB than those of the time-domain filtered m-sequences. This is also true for all the crosscorrelation values. The lower off-peak autocorrelation and crosscorrelation values mean that the frequency domain-filtered m-sequences are closer to being orthogonal for the purposes of simultaneous multi-sourcing.

Figure 24 displays numerically-simulated blended uncorrelated data for one receiver line and four vibrators running simultaneously. The separation between adjacent vibrators was 400m, and the receiver line was offset from the source line by 5m. Figure 24(a) was produced using the time-domain-filtered set of m-sequences as pilots. Figure 24(b) was produced using the frequency-domain-filtered set of m-sequences as pilots. The appearances of the two blended gathers of uncorrelated data are very similar, and no distinguishing features exist to give reason for preferring one over the other.

Deblended common-source gathers of seismograms were extracted from the blended raw data by crosscorrelating with the appropriate m-sequence pilots. Figure 25(a) displays the numerically simulated CSGs produced using the time-domain-filtered m-sequence pilots, and we see strong artifacts and a high level of crosstalk interference that obscures the reflected arrivals. However, on Figure 25(b) displaying the simulated CSGs produced using the frequency-domain-filtered m-sequence pilots, the artifacts and crosstalk have been reduced to near invisibility.

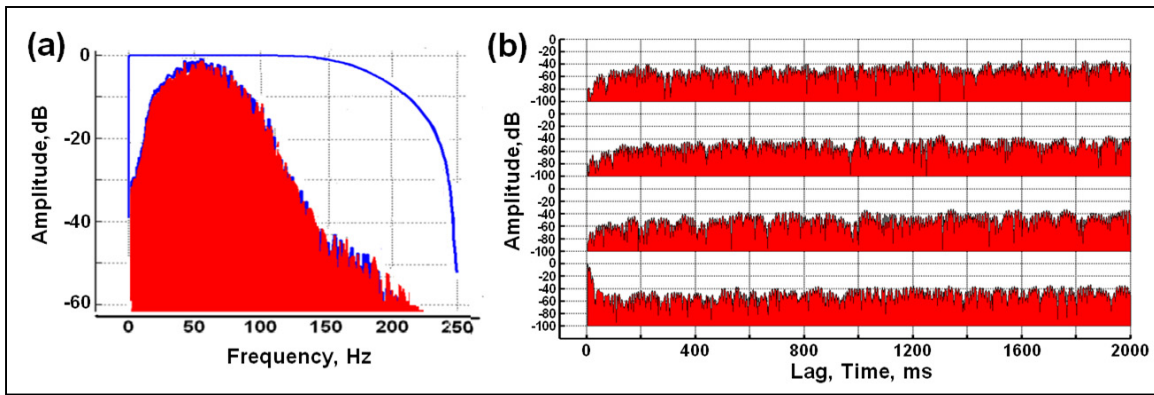


Figure 22: (a) Blue = spectrum of unfiltered m-sequences. Red = spectrum of time-domain filtered m-sequences (b) Bottom trace is autocorrelation of time-domain filtered m-sequences, top three traces are their crosscorrelations.

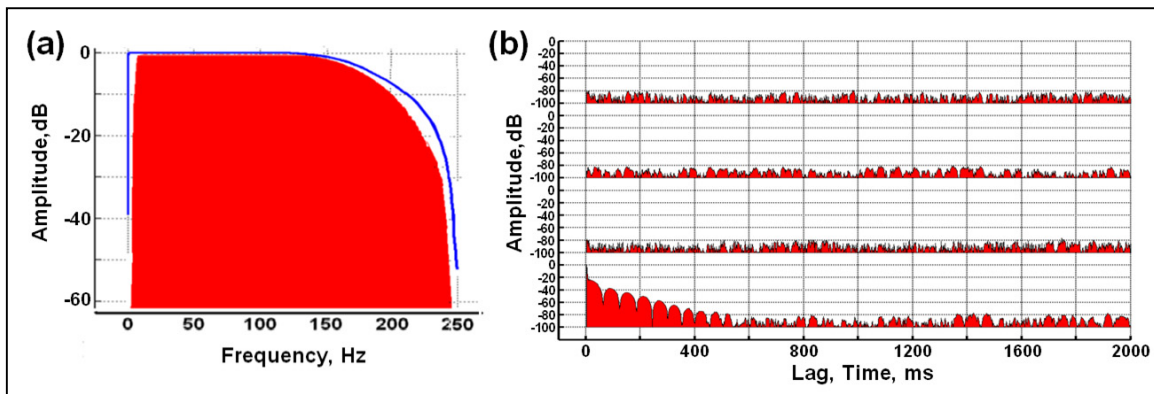


Figure 23: (a) Blue = spectrum of unfiltered m-sequences. Red = spectrum of frequency-domain filtered m-sequences (b) Bottom trace is autocorrelation of frequency-domain filtered m-sequences; top three traces are their crosscorrelations.

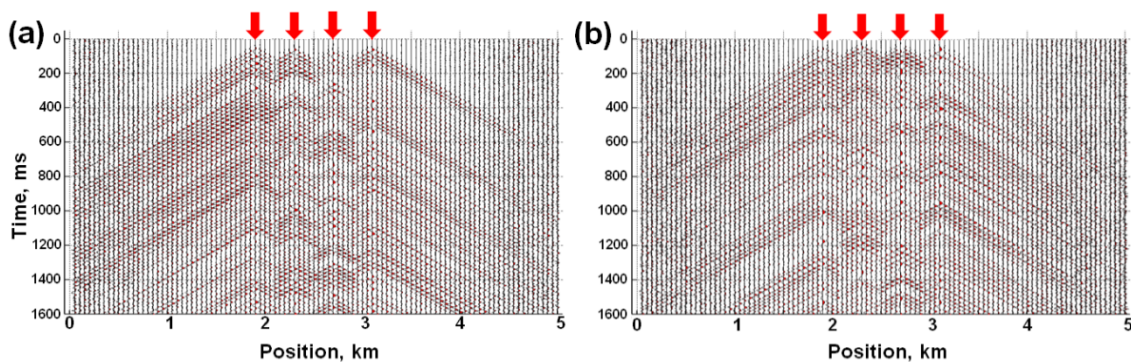


Figure 24: Trace-normalized plots of numerically simulated uncorrelated data for four simultaneous vibrators separated by 400m and 100 receivers separated by 50m. (a) Pilots used are time-domain-filtered m-sequences. (b) Pilots used are frequency-domain-filtered m-sequences.

For the time-domain filtered m-sequences, the drastic reduction in spectral content changes the mathematical properties of the pure m-sequences that enable them to approximate a perfectly orthogonal set so well (Wong, 2012a; 2012b). The reduction in spectral content is so severe that the time-domain filtered m-sequences are rendered much less effective for separating strong direct-arrival events and high-amplitude ground-roll signals from much weaker reflections.

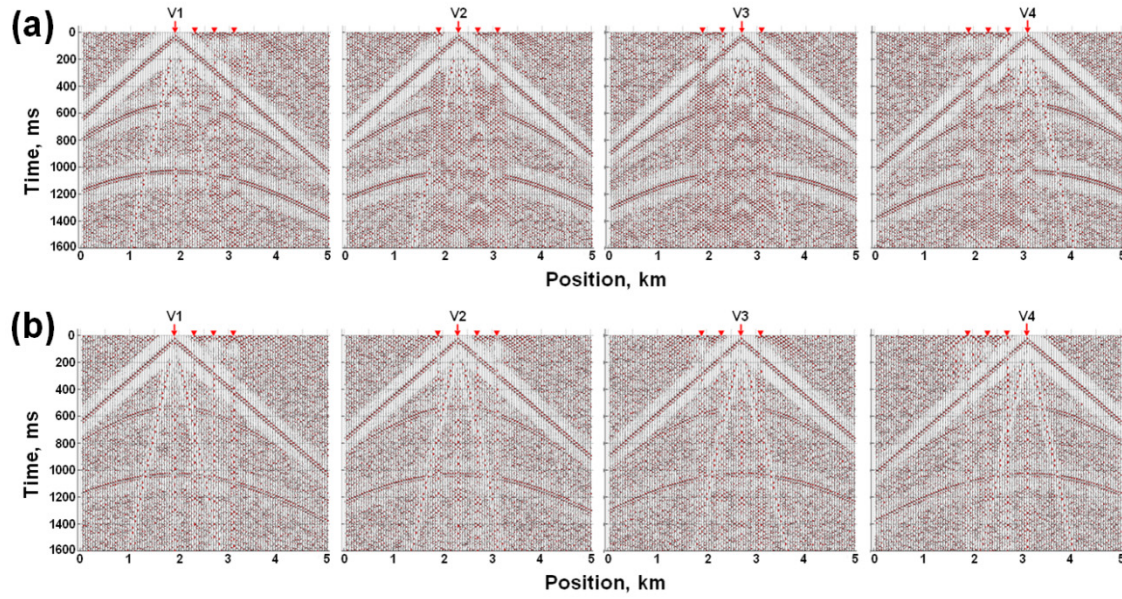


Figure 25: (a) AGC plot of deblended CSGs simulated using the time-domain-filtered m-sequence pilots. (b) AGC plot of deblended CSGs simulated using the frequency-domain-filtered m-sequence pilots.

The frequency-domain-filtered m-sequences retained much more of the spectral energy of pure m-sequences in the frequency range 4 to 250Hz. Consequently, the reduction in the orthogonality of the m-sequence pilots is much less severe, and the associated deblended CGSs exhibit minimal levels of both artifacts and source-to-source crosstalk. The results of the numerical experiment point out the way to improve the deblending capability of filtered m-sequences: use bandpass filtering on pure m-sequences, and retain as large a band of spectral energy as is compatible with the mechanical responses of real vibrators. In practice, since the earth does not propagate seismic wave with frequencies above 100Hz for any great distance, we may need to set the high-frequency end of the compatible band to be considerably less than 250Hz, especially when 2ms sampling rates are used for field acquisition. Also, since ground roll (with dominant frequencies of 20 Hz and less) is a major source of noise relative to reflected events (with dominant frequencies on the order of 40-50Hz), we may be able to reduce ground roll interference by limiting the low-frequency energy content of the filtered m-sequence pilots, thereby assigning higher vibrator output to the frequencies that characterize reflections.

CONCLUSION

A field test involving a single vibrator has verified that shifted m-sequences modified by a time-domain filter can control land vibrators successfully. The results show that the quality of seismograms acquired with filtered m-sequence pilots compares favorably with the quality of seismograms acquired with standard linear sweep pilots. Weak reflections on seismograms acquired using m-sequence pilots are somewhat degraded by low-amplitude artifacts. The artifacts have predictable time moveouts that run parallel to the first arrivals, and simple processing steps can reduce them to a level where their interference with the weaker reflections is minimal.

We also assessed the suitability of time-domain filtered m-sequences as pilots for simultaneous multi-vibrator acquisition. Using two vibrators separated by 200m and four vibrators separated by 100m, we recorded blended uncorrelated data from which we obtained ordinary common-source gathers by crosscorrelating with the quasi-orthogonal m-sequence pilots. Reflection events on the deblended seismograms are somewhat degraded by weak artifacts and weak crosstalk interference. The crosstalk originates from high-amplitude first arrivals and surface waves coming from nearby and adjacent vibrators, and is strongest for receivers located close to the vibrator sources. For receiver lines far away from the vibrator locations, first-arrival and surface-wave amplitudes from nearby vibrators are not overwhelmingly stronger than the arrivals from the vibrator of particular interest. As a result, the crosstalk interference after crosscorrelation for these lines is much less. Simple processing techniques were successful in attenuating the artifacts and crosstalk and in enhancing the reflections.

We used numerical simulations to study the effect of bandwidth of filtered m-sequences on their effectiveness used as pilot signals in simultaneous multi-vibrator acquisition. The simulations indicate that filtered m-sequences may be optimized for practical simultaneous multi-sourcing if their energy is concentrated in the 4-100 Hz pass band.

The following main conclusions can be drawn from our field and numerical investigation:

1. Hydraulically-powered land vibrators can be controlled successfully by filtered m-sequences.
2. Quasi-orthogonal filtered m-sequences are effective pilots for simultaneous source acquisition with two or four vibrators.
3. The deblending capability of quasi-orthogonal filtered m-sequences pilots used in simultaneous multi-source acquisition is improved
 - (a) if the source interval is decreased to 100 or 50 meters, and
 - (b) if the pass band of the filtered m-sequences is adjusted to match the pass band of the earth response.

ACKNOWLEDGMENTS

We thank Devon Energy Corporation for permission to present these results. Keith Radcliffe and Tom Phillips assisted in setting up the filtered m-sequence pilots for the vibrator controllers. CREWES is supported financially by its industrial sponsors, and also is funded the Natural Sciences and Engineering Research Council of Canada (NSERC) through Grant CRDPJ-461179-13.

REFERENCES

- Bagaini, and Ji, Y., 2010, Dithered slip-sweep acquisition: 80th International Annual Meeting, SEG, Expanded Abstracts, pp. 91-95.
- Beasley, C., 2008, A new look at marine simultaneous sources: *The Leading Edge*, **27**, 914-917.
- Bouska, J., 2010, Distance separated simultaneous sweeping for fast clean vibroseis acquisition: *Geophysical Prospecting*, **58**, 123-153.
- Dean, T., 2014, The use of pseudorandom sweeps for vibroseis surveys: *Geophysical Prospecting*, **62**, 50-74.
- Krohn, C., Johnson, M., Ho, R., and Norris, M., 2010. Vibroseis productivity: shake and go, *Geophysical. Prospecting*, **58**, 102-122.
- Pecholcs, P., Lafon, S. K., Al-Ghamdi, T., Al-Shammery, H., Kelamis, P. G., Huo, S. X., Winter, O., Kerboul, J.B., and Klein, T., 2010, Over 40,000 vibrator points per day with real-time quality control: opportunities and challenge: 80th International Annual Meeting, SEG, Expanded Abstracts, **29**, 111-115.
- Sallas, J., Gibson, J., Maxwell, P., and Lin, F., 2011, Pseudorandom sweeps for simultaneous sourcing acquisition and low-frequency generation: *The Leading Edge*, **30**, 1162-1172.
- Thomas, J.W., Jurick, D.M., and Osten, D., 2012, Vibroseis as an impulsive seismic source - 3D field testing Permian Basin Texas: 80th International Annual Meeting, SEG, Expanded Abstracts, 86-90.
- Thomas, J.W., Chandler, B., and Osten, D., 2010, Galcode: simultaneous seismic sourcing: 80th International Annual Meeting, SEG, Expanded Abstracts, 86-90.
- Wong, J., 2013, Multiple simultaneous vibrators controlled by m-sequences: 83rd Annual International Meeting, SEG, Expanded Abstracts, 109-113.
- Wong, J., 2012a, Simultaneous multi-source acquisition using m-sequences: CREWES Research Report, **25**, 81.1-81.16.
- Wong, J., 2012b, Spread spectrum techniques for seismic data acquisition: CREWES Research Report, **25**, 82.1-82.20.
- Wong, J., and Langton, D., 2014, Simultaneous multi-source acquisition using m-sequences: CREWES Research Report, **26**, 81.1-81.16.
- Wong, J., and Langton, D., 2015, Multiple simultaneous vibrators controlled by m-sequences: CSEG Geoconvention, Calgary, Expanded Abstracts.